J. Fluid Mech. (1987), *vol.* 181, *pp.* 387–413
Printed in Great Britain

The interaction of turbulence and pressure gradients in a baffle-stabilized premixed flame

By M. V. HEITOR†, A. M. K. P. TAYLOR AND J. H. WHITELAW
Department of Mechanical Engineering, Imperial College, London SW7 2BX, UK

(Received 7 July 1986 and in revised form 3 February 1987)

Simultaneous measurements of time-resolved velocity and temperature have been obtained by laser-Doppler anemometry and numerically compensated fine-wire thermocouples in the near wake of a premixed flame stabilized on a disk baffle located on the axis, and at the exit, of a confining pipe. The diameter of the disk was 0.056 m, the diameter of the pipe was 0.080 m, the volumetric equivalence ratio with natural gas as the fuel was 0.79 and the Reynolds number, based on pipe diameter and upstream pipe bulk velocity of 9 m/s, was 46800. The purpose of the measurements is to quantify the relative magnitudes of terms involving the mean pressure gradient and Reynolds stresses in the balance of turbulent kinetic energy and heat flux in a strongly sheared, high-Reynolds-number, reacting flow. The latter term has been associated with non-gradient diffusion in other flows. Source terms involving the mean pressure gradient are large in the conservation of turbulent heat flux but not in the conservation of Reynolds stress. The 'thin-flame' model of burning suggests that the sign and magnitude of the heat flux is closely related to the conditioned mean velocities. The mean axial velocity of the reactants is larger (by up to 0.27 of the reference velocity) than that of the products on the low-velocity side of the shear layer that surrounds the recirculation bubble but the reverse is true on the high-velocity side. These observations are related to the sign of the axial pressure gradient, which is associated with the streamline curvature, and the consequent preferential acceleration of the low-density products. Generally, the Reynolds stresses of the products are higher than those of the reactants and, in contrast to previously reported measurements, the contribution to the unconditioned stresses by the difference in the mean velocity between products and reactants, the so-called 'intermittent' contribution, is small. This is a consequence of the high Reynolds number of our flow.

1. Introduction

In turbulent, premixed flames there arise source terms, explicitly set out below, in the conservation equations for the turbulent heat transfer rate and stresses that have no counterparts in non-reacting flows. Analysis (Masuya & Libby 1981; Bray, Libby & Moss 1985; Libby 1985) has shown that at least in the two idealized extremes with the flame either normal or oblique to the approaching reactants, and at practically important levels of heat release, these terms are sufficiently large to cause non-gradient transport of turbulent heat flux. This finding is important because it casts doubt on the applicability of turbulence models that use the gradient-transport hypothesis. Similar effects can be observed in non-premixed flames, as shown by

† Now at the Instituto Superior Técnico, Mechanical Engineering Department, Lisbon, Portugal.

Stårner & Bilger (1980, 1981) and Stårner (1983). The extra terms in the equations for the transport and Reynolds stress involve the mean pressure gradient and can act as sources or sinks of turbulence and make significant contributions to the change in turbulent kinetic energy as the flow crosses the flame front. As pointed out by a reviewer, terms that involve pressure fluctuations, such as $-\overline{c'' \partial p'/\partial x_i}$, are potentially as important as those that include the mean pressure gradient, although Masuya & Libby (1981) have advanced the argument that the neglect of the redistributive effects of pressure fluctuations within the reaction zone may be defensible because this is thin for premixed flames. Our attention to the terms that contain the mean pressure gradient reflects the notorious difficulty attached to measurements of fluctuating pressure. Another result is that the mean streamline directions of the reactants and products are different from one another and from the mean streamline. This is due to the differential effects of gradients of mean pressure and Reynolds stresses on the heavy reactants and light products of reaction.

Measurements of the heat flux and one component of Reynolds stress have been made in weakly sheared unconfined (Shepherd & Moss 1981) and confined (Shepherd, Moss & Bray 1982) premixed flames that confirm the existence of non-gradient diffusion and the effect of production of turbulence due to the mean pressure gradient. Results have been obtained in sheared flames, such as V flames (Cheng, Talbot & Robben 1984; Cheng 1984) and the near-wall region of bunsen flames (Durst & Kleine 1973; Yoshida 1981), but, as is demonstrated by this work, these observations are not representative of higher Reynolds numbers such as that considered here.

The importance of these effects have been established in one-dimensional flow, where the generation of turbulence by shear strain has been either absent or weak. Arguments developed in such flows may not hold in sheared flows. The purpose of this paper is to examine the relative importance of source terms involving the gradients of mean pressures and Reynolds stresses in the balance of the turbulent kinetic energy and the turbulent heat fluxes and to determine the extent of non-gradient fluxes in a premixed flame stabilized on a bluff body. With the advantages of hindsight, these objectives may be expressed in greater detail as:

(*a*) to quantify the interaction between density fluctuations due to heat release and force fields due to gradients of mean pressure in the balance of turbulent kinetic energy, $-\overline{u_i''}\,\partial \bar{P}/\partial x_i$, and turbulent heat transfer rate, $-\overline{c''}\,\partial \bar{P}/\partial x_i$. Here, an overbar denotes a time-averaged quantity and a double prime denotes fluctuations from a density-weighted average: c is the fluctuation in the so-called 'reaction progress' variable, defined in the next section, and u_i is a component of fluctuating velocity;

(*b*) to identify the preferential effects of the forces referred to in (*a*) on the mean velocity of the low-density hot products relative to that of the high-density cold reactants;

(*c*) to examine the generation of turbulence by the flame by comparing the Reynolds stresses in the product gases with those in the reactant gases.

The near premixed flame considered here corresponds to a mixture of methane and air flowing along a pipe and over a disk baffle located on the pipe axis at its exit plane. The flame was stabilized on the baffle and was initially premixed with increasing influence of the external ambient air with distance downstream of the baffle. This arrangement was chosen because it allowed convenient access for the instrumentation, which comprised a laser-Doppler anemometer and a digitally compensated thermocouple.

The flow arrangement and instrumentation are described briefly in the following section. Further details, including consideration of possible error sources, have been

1 Watt (nominal) Argon-Ion laser: wavelength	514.5 nm
Beam diameter, at e^{-2} intensity, of laser	1.5 mm
Focal length of focusing lens	600 mm
Measured half-angle of beam intersection	2.88°
Calculated dimensions of measuring volume, at e^{-2} intensity (major and minor axis of ellipsoid)	5.19; 0.26 mm
Transfer constant	0.1946 MHz/m s^{-1}
Fringe separation (line-pair spacing)	5.1 μm
Focal length of collecting lens	200 mm
Magnification of receiving optics	1.56
Photomultiplier – pinhole aperture	0.34 mm

TABLE 1. Principal characteristics of the laser-Doppler velocimeter

provided by Heitor, Taylor & Whitelaw (1985) and Heitor (1985). The results are presented and discussed in §§3 and 4 respectively, in relation to the findings of previous work including that concerned with the modelling of flows with turbulent combustion. A summary of the more important conclusions is provided in §5. The detailed profiles of the results, from which contours were constructed, are to be found in Heitor (1985).

2. Flow arrangement and instrumentation

The flame was stabilized on a disk of diameter $d = 0.056$ m, which was positioned at the exhaust of a 1.83 m long straight pipe of diameter $D = 0.080$ m. Natural gas (94 % methane by volume) and air were mixed in a swirl register which presented an acoustically closed end: the resulting swirl was removed by a honeycomb which was followed by a flame trap constructed from screens. The experiences of Heitor, Taylor & Whitelaw (1984) confirmed that stable burning could be achieved in a range of equivalence ratios ϕ, defined as the volumetric fuel–air ratio relative to that for stoichiometric combustion, of around 0.6–1.1. A value of $\phi = 0.79$ was used here for which the corresponding adiabatic flame temperature T_{ad} is 1990 K and the heat release parameter, $\tau_H \equiv T_{ad}/T_0 - 1$, is 5.6 for T_0, the temperature of the approaching reactant stream, of 300 K. The Reynolds number, based on the pipe diameter and an average upstream velocity of 9 m/s, was 46800: the annular bulk velocity U_0 at the trailing edge of the disk was 18 m/s. The air flow was filtered to remove oil mist from the compressors and then seeded with powdered aluminium oxide of nominal diameter from 0.6 to 1.0 μm before agglomeration. The flow in the annulus formed by the disk and pipe was examined with laser velocimetry and detailed velocity characteristics near the trailing edge of the baffle have been provided by Heitor (1985).

Velocity was measured by a dual-beam, forward-scatter arrangement with sensitivity to the flow direction provided by light-frequency shifting from acousto–optic modulation (Bragg cells) at 40 MHz: the remaining principal characteristics are given in table 1.

The scattered light was collected by a lens and focused onto the pinhole aperture (0.34 mm) of a photomultiplier with magnification of 1.56. The output of the photomultiplier was mixed with a signal derived from the driving frequency of the Bragg cell to give a net frequency up to 9 MHz. The signal was amplified (20 dB), measured by a frequency counter and passed to a 16-bit laboratory minicomputer with 32 k storage words.

Temperature was measured with thermocouple junctions made by butt welding platinum wires with platinum–rhodium (13%) wires of either 40 or 15 μm diameter, so that the aspect ratio of the wire was over 200, which rendered conductive heat loss from the beads negligibly small (Bradley & Matthews 1968). The thermocouple was mounted on a straight length of twin-bore ceramic cladding (2.5 mm diameter) and located about 1 mm downstream of the measuring volume of the anemometer, at an angle of 22° to the optical axis. The probe was not observed to act as a source of flame stabilization when introduced into the flow. Heat loss from the thermocouple by radiation results in underestimation of the mean temperature by up to 150 K. The time-resolved temperature is also affected by this loss but the corresponding effect on the time constant of the thermocouple is unimportant (less than 10%; see Ballantyne, Boon & Moss 1976) in comparison with the other sources described by Heitor *et al.* (1985). Catalytic effects are also of secondary importance in this turbulent flame (see Heitor *et al.* 1985, for justification) in both mean and time resolved temperature and coatings were not applied.

The output of the thermocouple was differentially amplified (×100) and digitized by a 12-bit analogue-to-digital converter at sampling rates of up to about 38 kHz. The noise level could be kept below 0.098% of full-scale deflection, corresponding to a maximum temperature error of ± 2 K. The samples were initially stored in the memory of an 8-bit laboratory microcomputer with 48 k storage words and then passed to the larger minicomputer for data processing. The time constant for each thermocouple was measured as a function of velocity and corrected for temperature with a form of the law of Collis & Williams (1959). For the 15 μm wire, the bead size was taken into account by the correction of Moffat (1958). The resulting variation of time constant with temperature and velocity was recorded in the computer and for the measurements of the following section was in the range from 1.5 to 3.0 ms for the 15 μm wires and 5.5 times larger for the 40 μm wire. Compensation is required over 1.8 and 2.6 decades for the 15 and 40 μm wires respectively since the frequency response is expected to exceed 5 kHz and evidence for this, together with the reasons for the choice of seeding-particle concentration, wire diameter and calibration technique, are discussed by Heitor *et al.* (1985). The digital record of the temperature signal was compensated numerically in the minicomputer so that a simultaneous record of velocity and temperature could be obtained. Thus the probability function of each property and the joint probability function could be determined and, from these, the individual and joint moments. The population size varied with the measurement position but was usually between 1024 and 2560, leading to statistical errors in the unconditioned velocity characteristics below 1% and 7% for the mean and variance (Yanta & Smith 1978).

It was also possible to sample the velocity measurements conditionally according to the temperature (or vice versa). It is convenient in what follows to refer to the temperature as the 'reaction progress' variable:

$$C \equiv \left[\frac{T-T_0}{T_{ad}-T_0}\right],$$

where C and T denote instantaneous values. Here the conditioning levels were considered to be $C = 0.15$ ($T = 545$ K) for cold reactants and $C = 0.70$ ($T = 1480$ K) for hot products. The resulting estimates of the velocity moments are insensitive to these levels within 2 % and 8 % in the mean and variance respectively. The statistical inaccuracy can however be higher, depending on the population size of each point, and the random errors in the conditioned mean and variance of velocity are about 3 % and 15 %.

It is expected (see Heitor *et al.* 1985) that the laser velocimeter will measure a density-weighted velocity and that the thermocouple, because of its small size, will measure an unweighted temperature. However, when the temperature measurement is recorded only at the time of occurrence of a velocity signal, it too should be density weighted. The density-weighted probability functions are biased towards high velocities (McLaughlin & Tiederman 1973) but for the turbulence intensities considered here, the errors are less than +4 % and −4 % for the mean and variance respectively (Glass & Bilger 1978). The uncertainty associated with the measurement of turbulent heat flux $\widetilde{u_i c''}$, where the tilde denotes a density-averaged quantity, arises from a number of sources but the largest systematic error is due to the temperature-compensation procedure and is likely to be an underestimation of about 10 %. The largest random errors are due to the spatial separation of measurement locations of temperature and velocity and to the population size, and are of the order of 16 %. The resulting uncertainties in the measurements of conditioned and unconditioned velocities and the corresponding heat fluxes do not affect the conclusions to be drawn.

3. Results

This section presents the measurements of velocity and temperature–velocity correlations for the near wake of the disk. The purpose of the presentation is to compare and contrast the results with the corresponding non-reacting flow and with similar measurements that have been reported in other premixed flames. The results are presented as either profiles or contours, as appropriate. The latter have been drawn using linear interpolation between the measurements obtained along seven radial profiles, namely at $x/D = 0.38$, 0.50, 0.63, 1.00, 1.25, 1.50 and 2.50.

It is helpful to consider the nature of the flame under investigation before the presentation of the results and this can be achieved readily with the help of figures 1 and 2. Figure 1† shows that the thickness of the reaction surfaces, relative to the lengthscales of the packets of fully burned reactants and products in the reaction zone, is not negligibly narrow because the Damkoehler number is around 10. This number is defined as the ratio of characteristic timescales of the flow and chemical reaction, i.e. $D \equiv l/u' \; S_L/\delta_L$, where l is a measured turbulent lengthscale, u' denotes the r.m.s. velocity in the reactant stream, and laminar flame thickness and velocity are δ_L and S_L, respectively. It can be shown that if the reaction surfaces were negligibly narrow, the so-called 'thin flame' model of Bray *et al.* (1981), Masuya & Libby (1981), Bray *et al.* (1985) and Libby (1985), then the mean reaction rate would be independent of the chemical kinetics (Bray 1980). In our flame, it is likely that this approximation is worse than in the experiment of Shepherd *et al.* (1982) but better than in that of Bill *et al.* (1982). Wrinkled laminar flames can exist in a turbulent flow, according to the Klimov–Williams criterion, if the Kolmogorov microscale is greater than or equal to the laminar flame thickness. Since the conditions in our flow

† The lengthscale l was estimated in the manner of Shepherd & Moss (1983) using the conditional-sampling technique described by Heitor *et al.* (1985), and the results suggest asymmetric distributions with modal and mean values about 1 mm and between 5 and 10 mm respectively. Note that the value of viscosity at room temperature has been used.

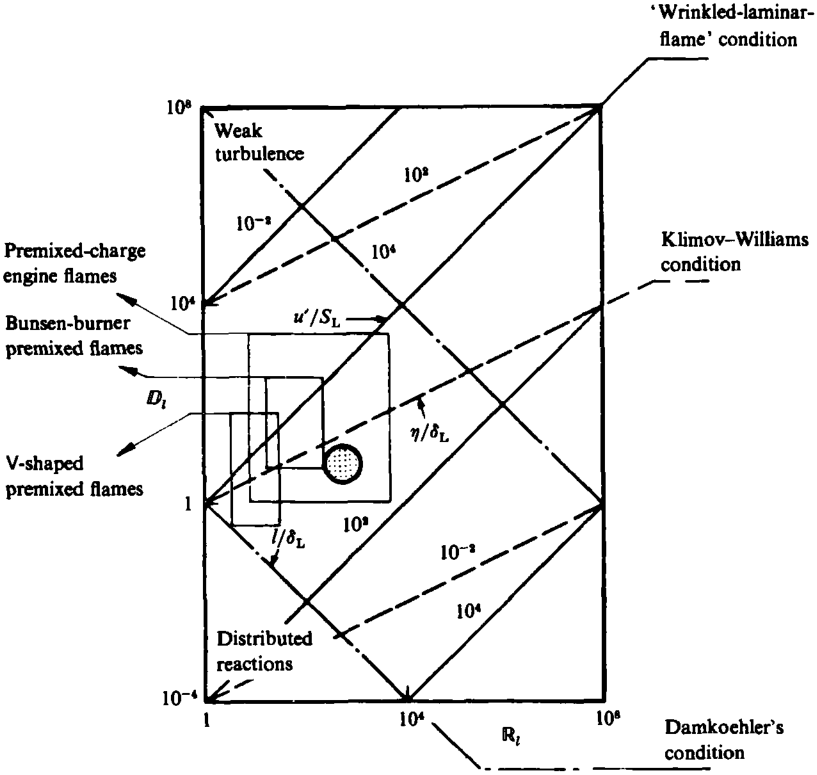

FIGURE 1. Illustration of regimes of turbulent combustion as a function of the Damkoehler (D) and Reynolds ($\mathbb{R}$) numbers, both based on a measured turbulent lengthscale l (after Williams 1984; Abraham, Williams & Bracco 1985). Circle identifies the combustion regime of the current experimental conditions on the basis of a Kolmogorov lengthscale $\eta = l\ \mathbb{R}^{-\frac{3}{4}} = 0.05$ mm. The laminar-flame thickness δ_L, and velocity S_L, are taken from Vinickier & van Tiggelen (1968) as 0.2 mm and 0.9 m/s, respectively; u' denotes the r.m.s. velocity in the reactant stream.

are such that the microscale, calculated on the basis of the viscosity of the cold reactants, is smaller than the laminar-flame thickness, we do not expect to have conditioned velocity characteristics similar to those of the V-shaped and bunsen-type premixed flames associated with wrinkled flame fronts, and this is confirmed by the work presented below.

Figure 2 show vectors of mean velocity and turbulent heat flux superimposed on isotherms: note that the subscript 0 refers to the approaching reactant stream. These are highly curved and, in the terminology of Masuya & Libby (1981) and Bray *et al.* (1985), reveal a non-planar flame oblique to the oncoming reactants. The reaction region occurs outside the locus of the mean separation streamline ($\psi = 0$) and is curved along its length. This curvature imposes mean velocity effects on the turbulence field and the result is a highly strained flame different from those for which detailed velocity and temperature measurements have been reported. The turbulent heat fluxes tend to be restricted to the shear layer with a large component directed along the isotherms so that non-gradient transport is likely.

The characteristics described above are considered in greater detail in the following paragraphs, which present profiles and contours of velocity characteristics. The discussion of §4 makes clear the implications for calculation methods.

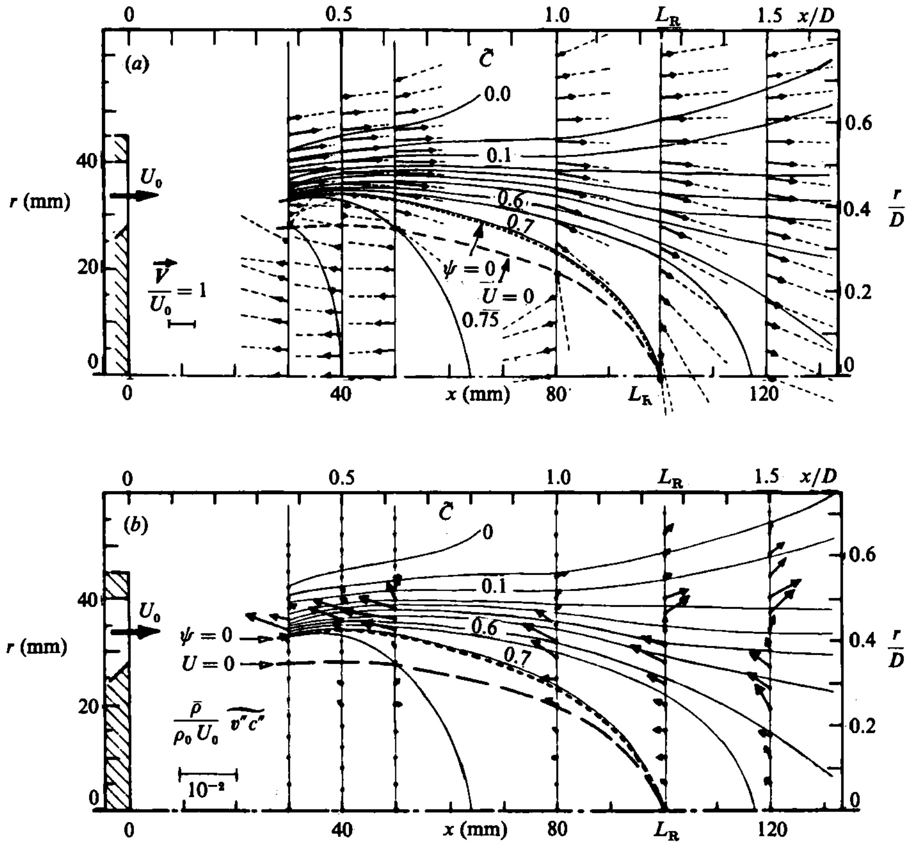

FIGURE 2. Vectors of (*a*) mean velocity, V/U_0, and (*b*) turbulent heat transfer rate, $\bar{\rho}\widetilde{v''c''}/\rho_0 U_0$, superposed on isotherms and separation streamline, locus $\psi = 0$. The scale for the magnitude of the vectors is given in the lower left-hand corner of each figure.

3.1. *Unconditioned velocity characteristics*

Some of the salient features of the flow are summarized conveniently by the centreline profiles of the mean velocity and Reynolds stresses for the reacting and non-reacting flows, figure 3. The recirculation length is longer in the combusting flow (in agreement with Clare *et al.* 1976; Fujii & Eguchi 1981; and Taylor & Whitelaw 1980), which also has higher reverse velocities; larger values of maximum turbulent kinetic energy occur in both flows at the rear stagnation point and there is a smaller recirculating mass flow rate. These results are likely to be strong functions of equivalence ratio, and opposite trends in recirculation length have been reported for confined flames by Winterfeld (1965) and Taylor & Whitelaw (1980) and for unconfined flames by Westenberg, Berl & Rice (1955). In common with other investigations in isothermal near wakes (Durão & Whitelaw 1978; Taylor & Whitelaw 1984) there is large anisotropy ($\widetilde{v''^2} > \widetilde{u''^2}$ where u and v denote the axial and radial components of velocity respectively), particularly at the rear stagnation point, but there is no evidence of any periodicity. This result is to be contrasted with the near wake of a plane baffle (Bradbury 1976) and with the recent measurements for axisymmetric disks at comparatively low velocities (Castro 1985). The probability-density distributions of the centreline axial velocity for the reacting flow immediately upstream

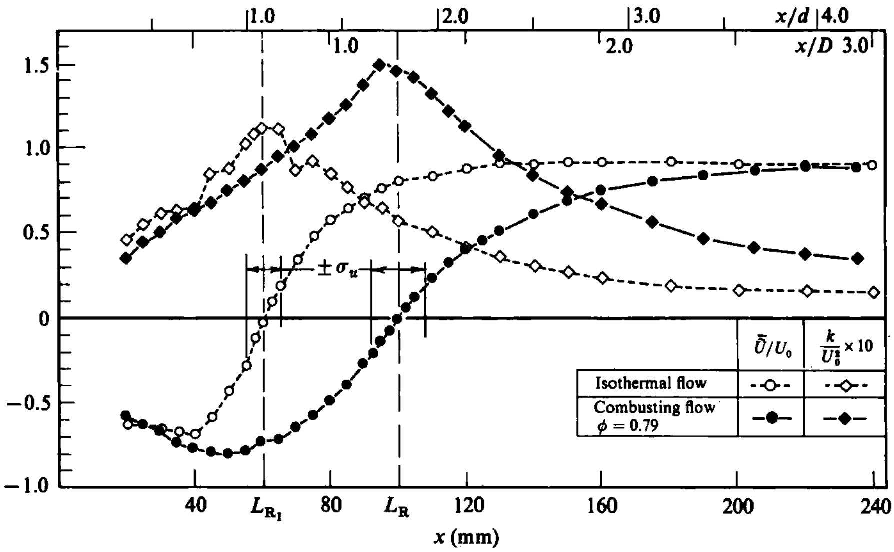

FIGURE 3. Centreline values of mean axial velocity and turbulent kinetic energy for isothermal and reacting flow. Baffle diameter is d, confining pipe diameter is D; U_0 is the annular bulk velocity; σ_u is the standard deviation in the length of the recirculation zone and ϕ is the volumetric equivalence ratio. $L_R = 100$ mm $= 1.25D = 1.75d$; $L_{RI} = 60$ mm $= 0.75D = 1.07d$.

and downstream of the stagnation point ($L_R \pm 0.50\ D$, where L_R denotes the length of the recirculation zone and $D = 0.08$ m is the diameter of the confining pipe) are skewed (0.5 and -0.5 respectively) and have high flatness (> 4). The present results do not provide evidence that can decide between theories of 'eddy splitting' at the stagnation point (Bradshaw & Wong 1972) or upstream/downstream 'deflection' of eddies (Kim, Kline & Johnston 1978).

The radial distributions of the velocity characteristics are also qualitatively similar for non-reacting and reacting flows. Profiles taken in the plane of the baffle show that the streamlines near the edge are at a larger inclination in the reacting flow, with the result that the maximum width of the recirculation zone is wider (by about 20 %). The axial velocities are higher, as expected owing to the expansion of the gases, by about 16 % in the axial plane containing the maximum velocities. The spreading rate of the boundary of the annular jet (defined as the radial location at which the axial velocity falls to one-tenth of the maximum value of the radial profile) is about 0.14 compared to about 0.09 for non-reacting round jets (see Ribeiro & Whitelaw, 1980a) and suggests significant entrainment of the ambient air. This spreading and the cooling effect of the disk result in a decrease of the mean temperature along the centreline, with differences from the adiabatic flame temperature of about 515 K ($0.25T_{ad}$) at stagnation. These considerations do not affect the conclusions that are drawn from the results.

The distributions of the components of the Reynolds stress tensor, figure 4, are similar to those in non-reacting, confined flows (e.g. Taylor & Whitelaw 1984) in that $\widetilde{v''^2}$ and $\widetilde{w''^2}$, where w denotes the azimuthal component of fluctuating velocity, are the largest stresses with the maxima located near the rear stagnation point, while the highest values of $\widetilde{u''^2}$ lie along the shear layer at $r/R \approx 0.5$, where $R = 0.040$ m is the radius of the confining pipe. The sign of the shear stress $\widetilde{u''v''}$ is related to the sign of the shear strain $\partial \tilde{U}/\partial r$ in accordance with a turbulent viscosity hypothesis ($\widetilde{u''v''} = -\nu_T \partial \tilde{U}/\partial r$ where ν_T is a scalar turbulent viscosity) except for a narrow zone in the region where the shear strain is close to zero, which is also found in non-reacting recirculation flows (e.g. Durão & Whitelaw 1978; Fujii, Gomi & Eguchi 1978; Durão, Durst & Firmino 1984). It is noted, however, that large regions of *counter*-gradient shear stress can be found in both V-shaped premixed flames (e.g. Cheng & Ng 1983; Cheng 1984) and bunsen-like flames (e.g. Durst & Kleine 1973; Yoshida 1981). This observation receives further attention in §3.2.

We have addressed the question of whether the nature of the turbulence has changed owing to combustion in the following three ways. First, the shear stress has been normalized by the maximum axial velocity in each profile, $\widetilde{u''v''}/U^2_{max}$, where U_{max} is the maximum axial velocity at the axial station. At the location of the stagnation point, where the maximum radial variation of $\widetilde{u''v''}/U^2_{max}$ is found, these values varied from -0.026 to 0.019 and from -0.022 to 0.013 in the reacting and non-reacting flows respectively. For comparison, Durão & Whitelaw (1978) reported values in a similar, non-reacting annular jet of between -0.010 within the recirculation zone and 0.018 downstream of the stagnation point: Townsend (1976) reports the value of 0.025 for jets; and Etheridge & Kemp (1978) measured values up to -0.019 upstream of the reattachment of a backstep isothermal flow. Secondly, the correlation coefficient for the shear stress is found to vary between -0.4 and -0.6 in the shear layer surrounding the baffle, and 0.45 and 0.6 in the outer flame zone. Thirdly, the shear stress has been normalized by the turbulent kinetic energy and the values lie between -0.35 and 0.30, which is close to the value expected in 'normal' shear layers (e.g. Bradshaw, Ferriss & Atwell 1967; Harsha & Lee 1970). All three criteria suggest that the shear stress in our reacting flow is similar to that in the isothermal flow and that therefore the influence of the extra terms in the conservation equations for Reynolds stresses is minor.

3.2. *Conditioned-velocity characteristics*

The unconditioned and conditioned radial profiles of mean axial velocity are presented in figure 5(*a*) and it is evident that reactants and products initially coexist only in a thin layer around the maximum axial velocity, and only far downstream ($x/D > 2.5$) do the two states coexist at the centreline. In addition, the mean axial velocity of the products is usually (see below) smaller than that of the reactants, with mean differences around $0.15U_0 = 2\ \mathrm{m\ s^{-1}}$ and maximum difference of $0.27U_0$, where U_0 is the bulk annular velocity in the plane of the exit of the confining pipe. Most other measurements of conditioned velocity in premixed flames have shown product axial velocities larger than those of the reactants, e.g. the bunsen flames of Shepherd & Moss (1981), the confined, step-stabilized flame of Shepherd *et al.* (1982) and the V-shaped flames of Cheng (1984) and Cheng *et al.* (1984). The difference is probably due to the large adverse axial gradients of pressure that are associated with the recirculation zone, and this point is discussed further in §4. The few exceptions in our flow where the products have a higher velocity that the reactants are to be found near the outer edge of the annular jet downstream of $x = 1.25D$. In conjunction with the profiles of radial velocity, it is found that the products are deflected away from the centreline, relative to the reactants, with an angle of 1°–5° between the two states.

The conditioned and unconditioned profiles of the density-averaged turbulent kinetic energy and shear stress are shown in figure 5(*b*, *c*). Qualitatively the conditioned profiles for both quantities are similar, with the shear stress in the

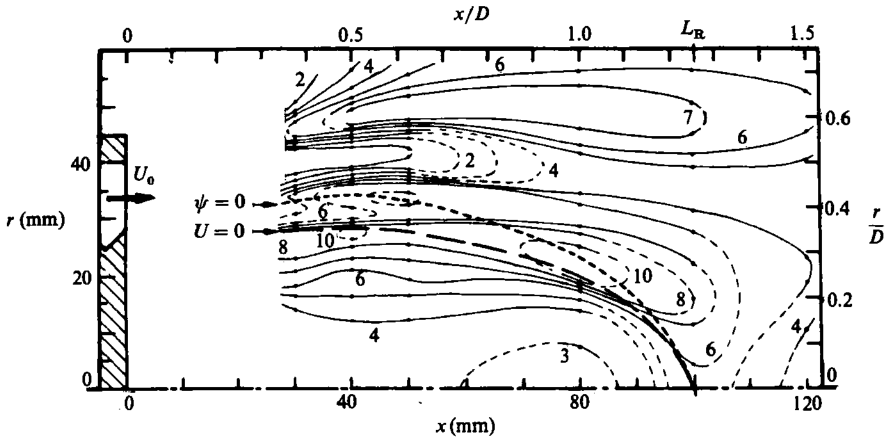

(*b*)

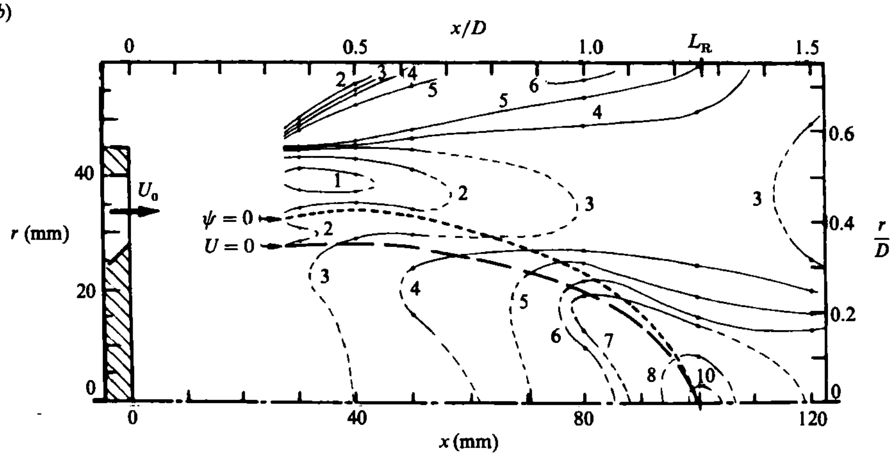

(*c*)

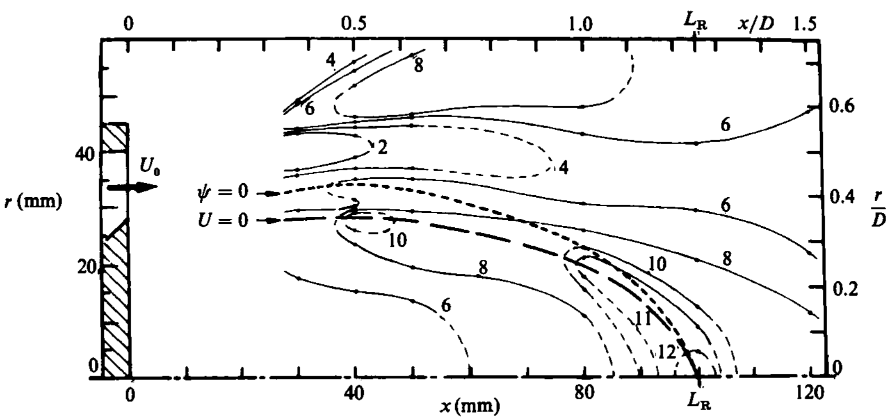

FIGURE 4(*a–c*). For caption see facing page.

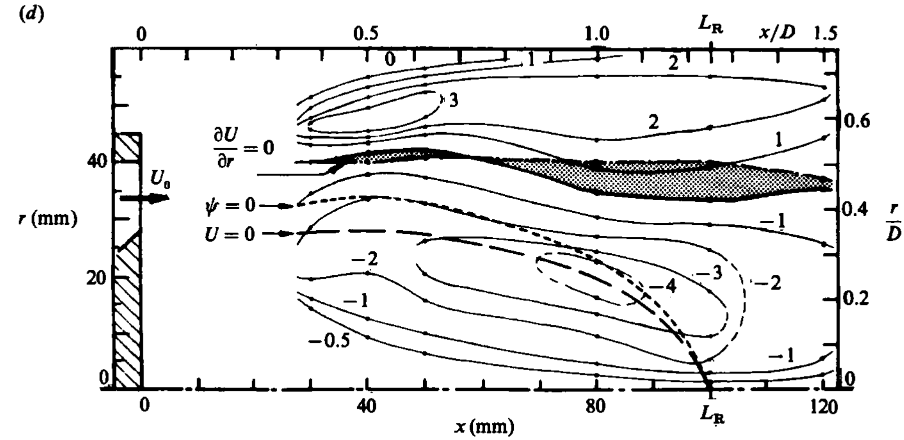

FIGURE 4. Contours of Reynolds stresses (*a*) axial component $100\widetilde{u''^2}/U_0^2$; (*b*) radial component $100\widetilde{v''^2}/U_0^2$; (*c*) turbulent kinetic energy $100\tilde{k}/U_0^2$; (*d*) shear stress $100\widetilde{u''v''}/U_0^2$: shaded regions show areas where the turbulent-viscosity hypothesis is untenable because the sign of the shear stress is the same as that of shear strain.

reactants higher by about $0.01 U_0^2$ than in the products, and the opposite is true for turbulent kinetic energy, except at $x/D = 1.25$, as discussed below, where the products are greater by about $0.02 U_0^2$.

It is convenient to refer to the work of Bray *et al.* (1985) who show that

$$\widetilde{u_i'' u_j''} = \tilde{C}(\overline{u_i u_j})_P + (1-\tilde{C})(\overline{u_i u_j})_R + \tilde{C}(1-\tilde{C})(\bar{U}_{iP} - \bar{U}_{iR})(\bar{U}_{jP} - \bar{U}_{jR}), \qquad (1)$$

where the subscripts P and R denote conditioned quantities in the product and reactant gases respectively and where the main approximation in this equation is that the probability of intermediate burning states is small (in other words, that the 'thin flame' approximation holds). The first two terms on the right-hand side of (1) are turbulent contributions to the unconditioned density-averaged Reynolds stresses but the final term is a non-turbulent (see Bray *et al.* 1981), or 'intermittent' contribution. For example the third term contributes less than around 10% to $\widetilde{u''^2}$ with a maximum value of about 22% in the vicinity of the location of the maximum width of the recirculation zone. Once more, this result is in contrast to published work in unconfined bunsen flames (Shepherd & Moss 1981), confined flames (Shepherd *et al.* 1982) and particularly the V-shaped flames of Cheng *et al.* (1984) and Cheng (1984) where the 'intermittent' contribution was the largest to the measured unconditioned stresses. The result is also in contrast to the analysis of unconstrained (Bray *et al.* 1981) and constrained (Masuya & Libby 1981) oblique normal flames where, again, the difference in the mean velocity within the reactants and products was dominant. Cheng (1984) presents evidence that associates counter-gradient shear stress with the intermittent contribution (so-called 'flapping' flames), and Moss (1980) has suggested that the intermittency occurs only at low Reynolds numbers. We conclude that intermittency is unimportant in our flow. The major role played by the conditioned turbulence in the flame is a striking feature differentiating this premixed flame from those mentioned above, but we should emphasize that this conclusion applies only to the Reynolds stresses and not to the turbulent heat transfer rate.

Results along an axial profile at $r/D = 0.46$, figure 6, show that the turbulent

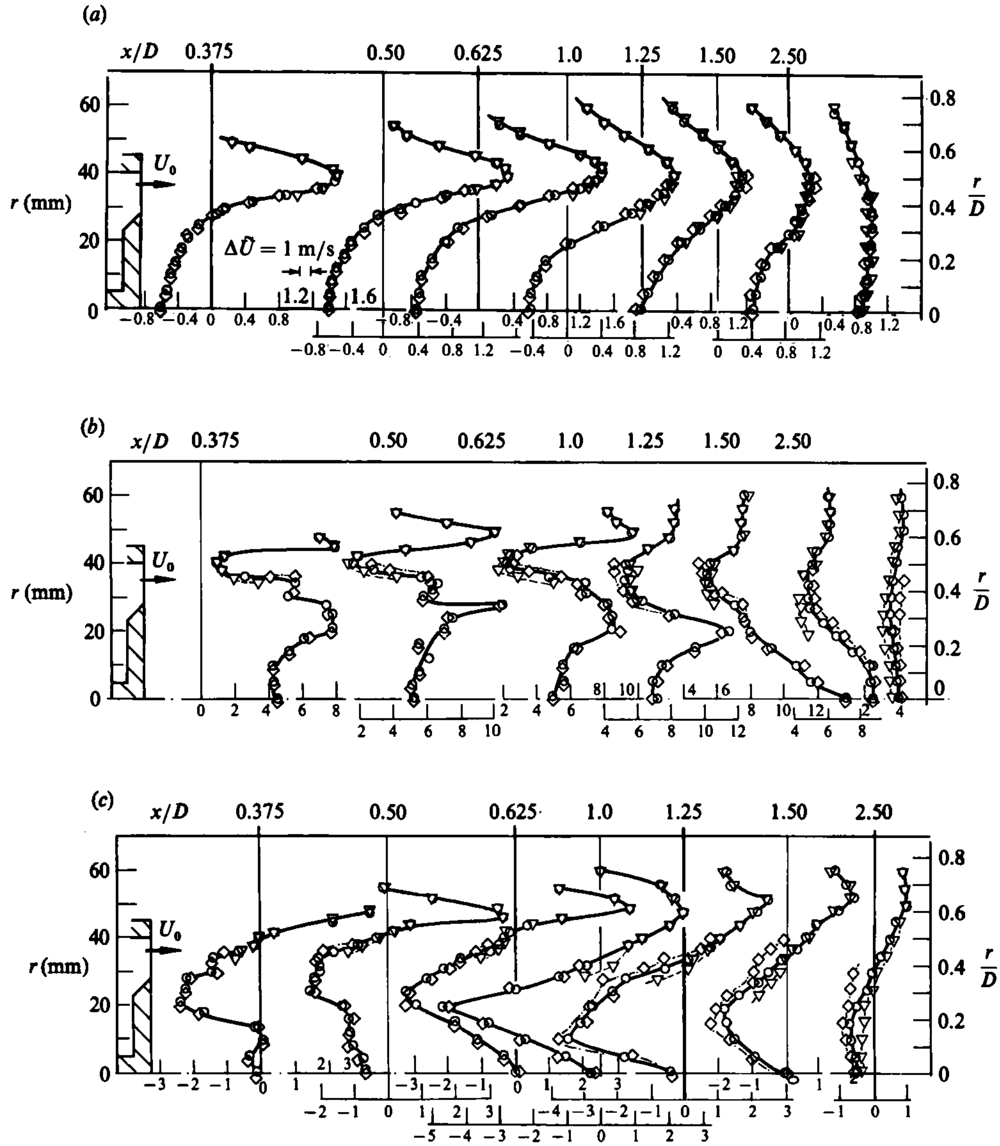

FIGURE 5. Radial profiles of velocity characteristics in unconditioned (○), reactant (▽) and product (◇) gases for (*a*) mean velocity $\tilde{U}/U_0$, (*b*) turbulent kinetic energy $100\,k/U_0^2$ and (*c*) shear stress $100\,\overline{u''v''}/U_0^2$.

kinetic energy of the product gases is higher than that of the reactants only upstream of $x = 0.69D$ ($= 55$ mm). Inspection of the contours of shear stress (figure 4*d*) suggests that this variation in the relative magnitude of the conditioned stresses is due to the proximity of the zone characterized by negative production of turbulence by shear stress. Further evidence is provided by the development of the shear-stress correlation coefficient along $r/D = 0.46$, figure 6(*b*), which should be analysed taking into account the shape of the radial profiles of figure 5(*c*). Despite the statistical errors that can arise from the small population size of the reactants in the downstream points, the increase in the absolute value of R_{uv} of the reactants relative to that of the products is remarkable downstream of $x/D = 0.69$. This set of results reveals the

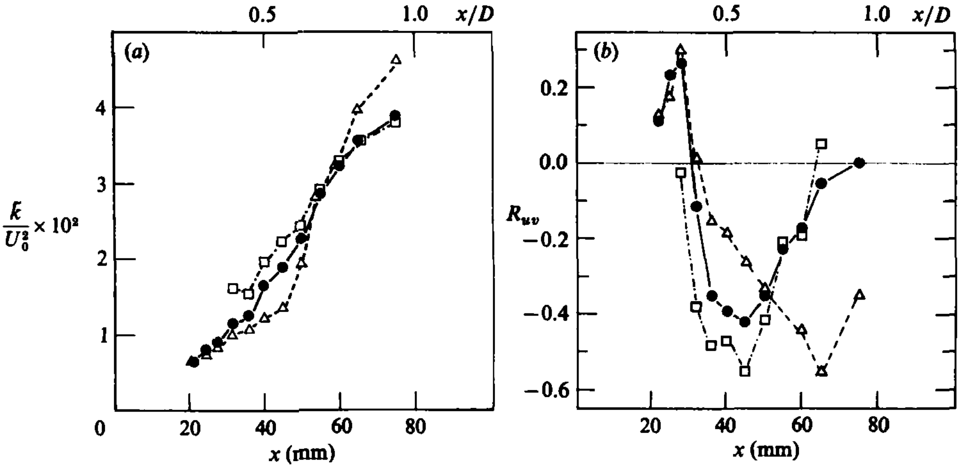

FIGURE 6. Axial profile along $r/D = 0.46$ of velocity characteristics in unconditioned (●), reactant (△) and product (□) gases for (*a*) turbulent kinetic energy and (*b*) shear-stress correlation coefficient.

importance of the shear-stress production term in the balance of turbulent energy and suggests that it may dominate the conditioned stresses, at least in strongly sheared flows. It is noted that, in contrast to the experimental investigations of Shepherd & Moss (1981), Shepherd *et al.* (1982), Cheng *et al.* (1984) and Cheng (1984) and the theoretical analysis of Masuya & Libby (1981), the present reactant stream is strongly sheared (i.e. $\overline{uv}_R \neq 0$) so that the behaviour described above is not surprising.

The calculations for planar flames carried out by Bray *et al.* (1981) and Masuya & Libby (1981) have avoided the use of gradient-transport hypotheses, such as those used in non-reacting flows. Closure for turbulent transport has been achieved by relating the conditioned variances within the reactants and products to the conditioned mean velocities as follows:

$$\frac{\overline{u_{iP}^2}-\overline{u_{iR}^2}}{(\overline{U}_{iP}-\overline{U}_{iR})^2} = \text{constant}. \tag{2}$$

This hypothesis is not supported by the data of Moss (1980), as shown by Bray *et al.* (1981), but Cheng *et al.* (1984) report qualitative agreement with the extension of the above equation:

$$\frac{k_P - k_R}{(\overline{U}_P-\overline{U}_R)^2} = \text{constant}, \tag{3}$$

where k represents the turbulent kinetic energy, which for the present results does not have a quotient close to a constant. Bray *et al.* (1985) have suggested a revised model for the conditioned Reynolds stress:

$$(\overline{u_i u_j})_P - (\overline{u_i u_j})_R = [(1-K_{ij1})\tilde{C} + (K_{ij0}-1)(1-\tilde{C})]\widetilde{u_i'' u_j''}, \tag{4}$$

where $K_{ij1,0}$ are constants, which is a generalization of that shown by Libby (1985) to yield a theory of normal flames in better agreement with the results of Moss (1980) than (2). Although (4) does account for the change in the relative magnitude of the conditioned stresses, this is predominantly dependent on the local mean value of the

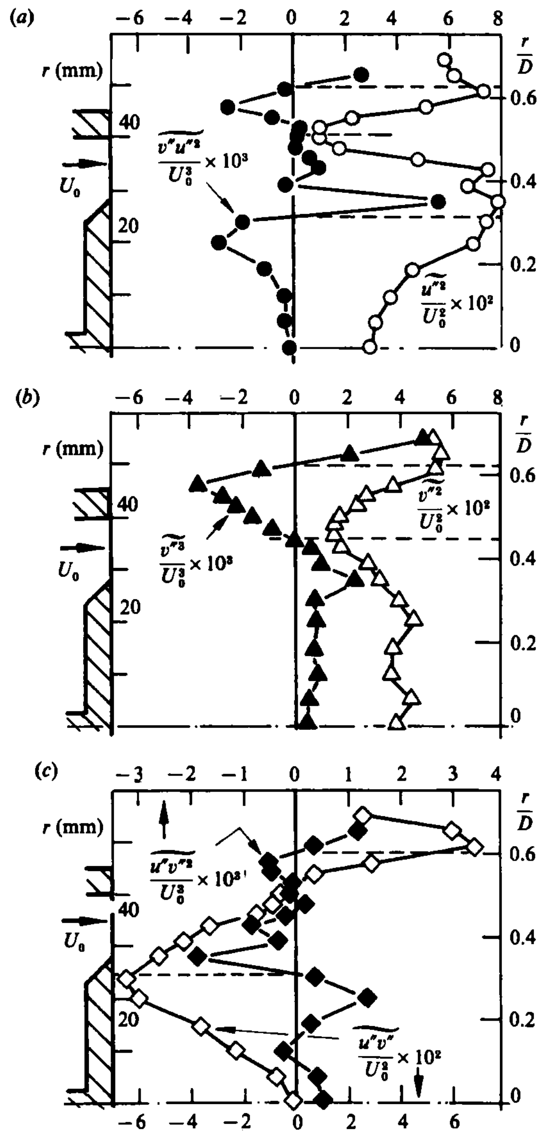

FIGURE 7. Radial profiles of triple velocity correlations near the location of maximum reverse velocity, at $x/D = 0.63$.

progress variable $\tilde{C}$. Our results do not support this model. It is interesting to note that the isotherm corresponding to $\tilde{C} = 0.5$ lies around the zone where the maximum differences between k_P and k_R have been observed and, therefore, precludes the case suggested by Libby (1985) for normal flames, of $K_{ij1} = K_{ij0}$ in (4) (note that under this condition $(\overline{u_i u_j})_P = (\overline{u_i u_j})_R$ if $\tilde{C} = 0.5$).

3.3. *Unconditioned triple-velocity products*

Diffusion of turbulent energy and shear stress may be associated with the gradients of triple-velocity products and has been attributed, e.g. by Castro & Bradshaw (1976) and Ribeiro & Whitelaw (1980*b*), to large-scale motion that is dependent on the surrounding field where both the Reynolds stresses and their gradients can change. In addition, the third-order correlations and hence turbulent diffusion are strongly affected by both longitudinal curvature and proximity of a stagnation zone. Figure 7 shows radial profiles at the location of the maximum width of the recirculation bubble of the triple products $\widetilde{u''^2 v''}$, $\widetilde{v''^3}$ and $\widetilde{u''v''^2}$, which represent the turbulent radial fluxes of $\widetilde{u''^2}$, $\widetilde{v''^2}$ and $\widetilde{u''v''}$ respectively. The correlations are qualitatively similar to those in the shear layer upstream of the reattachment zone and within the recirculation region in the backstep flows of Chandrsuda & Bradshaw (1981), Driver & Seegmiller (1983) and Pronchick & Kline (1983).

The distributions of figure 7 show that turbulent transport of both normal and shear stresses is mainly in the gradient sense. The triple products are zero at, or very close to, the points of zero radial gradient of the corresponding second-order correlations and their positive values are associated with turbulent transport of the Reynolds stresses from the high production-rate zones to the outer flow. The results also indicate large, positive and negative radial gradients of $\widetilde{v''u''^2}$ and $\widetilde{v''^3}$ around the edges of the annular jet which contribute to diffusive transport of turbulent energy. Further analysis is, however, reserved for §4 together with examination of the remaining terms in the conservation equation of turbulent kinetic energy. Nevertheless, it is noteworthy that the decrease of the third-order correlations near the centreline is far more rapid than the decrease of the shear- and normal-stress gradient. This behaviour agrees with that in the wall-bounded flow of Castro & Bradshaw (1976) and in the reattaching mixing layer of Chandrsuda & Bradshaw (1981) and has been explained by the dominance of large eddies in triple-product transport. The results suggest that calculation methods based on the hypothesis of gradient diffusion of turbulence energy and shear stresses will be inaccurate, at least near the centreline within the recirculation bubble.

3.4. *Turbulent heat flux*

Contours of the axial and radial turbulent heat flux are shown in figure 8 (azimuthal flux $\widetilde{w''c''}$ was measured and found to be zero, within experimental accuracy). These quantities represent the turbulent heat transfer rate (or, equivalently, the exchange rate of reactants), which is responsible for the phenomenon of flame stabilization around the recirculation zone and for flame propagation downstream of this zone.

The fluxes are largest within the thin reaction zone along the curved shear layer, as would be expected, although not spatially coincident with the zones of maximum turbulent kinetic energy. The radial heat flux is always positive – in other words, a heat flux directed away from the centreline. This is the expected direction in a baffle-stabilized flame since the ignition of the reactants (which are characterized by $c'' < 0$) must be associated with movement towards the recirculation zone ($v'' < 0$, hence net correlation $\widetilde{v''c''} > 0$). The flame is then established by the heat transfer between the hot products and the cold reactants. Note also that the sign of the radial heat flux is in qualitative agreement with gradient-transport models ($\widetilde{v''c''} = -\nu_c \partial\tilde{C}/\partial r$, where ν_c is a scalar turbulent thermal diffusivity).

Within the recirculation zone and for $x/D > 1$, the peak absolute values of the axial flux are larger by at least a factor of two than the values of the radial flux, even though the axial temperature gradients are negligible compared with those in the radial direction. The observation is not unusual, however, in the sense that similar ratios are found in heated, non-reacting flows such as curved boundary layers (Gibson & Verriopoulos 1984; Dakos, Verriopoulos & Gibson 1984), round jets (Chevray & Tutu 1978), coaxial jets (Johnson & Bennett 1983) as well as near the burner tip of the

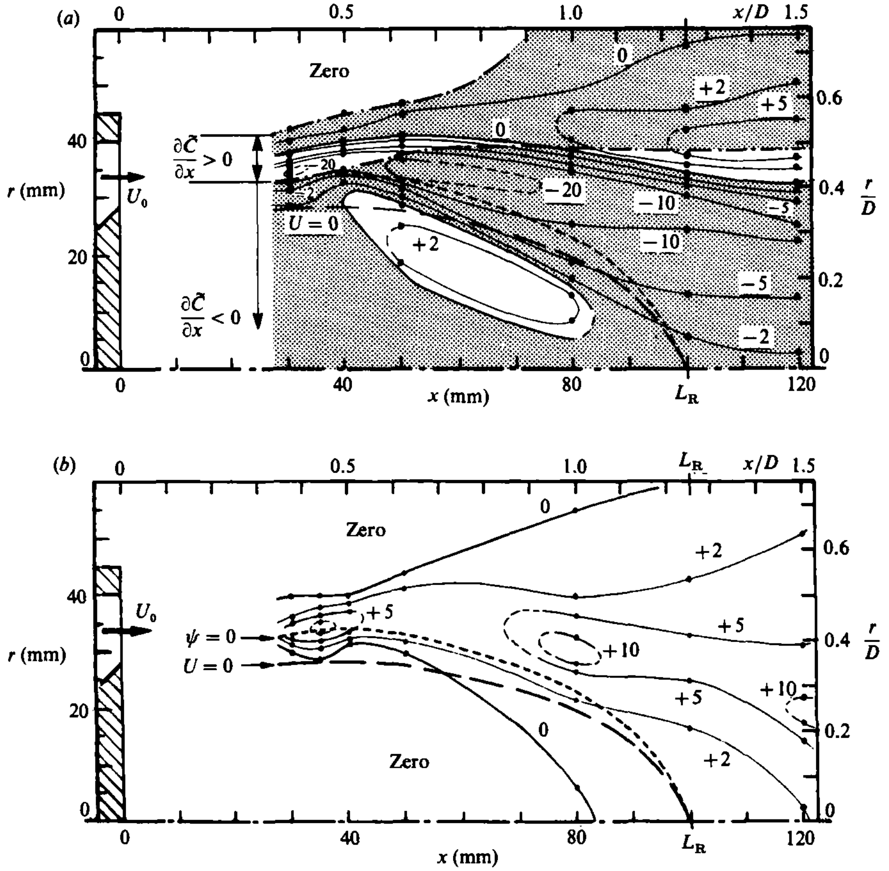

FIGURE 8. Contours of turbulent heat transfer rate: (*a*) axial heat flux $(1000\widetilde{u''c''}/U_0)$: shaded regions show areas of non-gradient axial transport where the sign of the heat flux is the same as that of the mean temperature gradient; (*b*) radial heat flux $(1000\widetilde{v''c''}/U_0)$.

premixed flame of Tanaka & Yanagi (1983). It should be recalled that it is the spatial gradients of the heat-flux components, and *not* the components themselves, that give rise to heat transport. The axial heat flux is directed towards the baffle, for $r/D < 0.5$, and is therefore directed against the sign of the axial gradient of mean temperature. Similar behaviour has been observed in other turbulent premixed flames (e.g. Moss 1980; Shepherd & Moss 1981; Shepherd *et al.* 1982; and Tanaka & Yanagi 1983) and has also been predicted analytically (Bray *et al.* 1981; Masuya & Libby 1981). The significance of the counter-gradient heat flux is that gradient-type models for turbulent heat flux are likely to be qualitatively incorrect in this region and is an important finding of our work.

The axial heat flux changes direction (i.e. sign) from negative to positive for $r/D > 0.5$. This change can be shown to be consistent with the change in the sign of the Reynolds shear stress $\widetilde{u''v''}$ at $r/D > 0.5$, as follows. Given that $\widetilde{v''c''}$ is found to be always positive, and that $\widetilde{u''v''}$ is positive for $r/D < 0.5$, this implies that on average hot products $(c'' > 0)$ move radially outwards (i.e. $v'' > 0$ because $\widetilde{v''c''} > 0$) and are associated with $u'' > 0$ (because $\widetilde{u''v''} > 0$). As consequence $\widetilde{u''c''}$ must be positive and this is confirmed by the measurements. For $r/D < 0.5$, the sign of $\widetilde{u''v''}$ is negative with the observed result that $\widetilde{u''c''}$ is also less than zero. It should be noted that in a V-shaped flame with a large intermittent contribution to the unconditioned Reynolds stress, Cheng & Ng (1983) and Cheng (1984) have shown different behaviour, with $\widetilde{u''c''} > 0$, $\widetilde{v''c''}$ and $\widetilde{u''v''} < 0$.

The radial profiles of the correlation coefficients (not shown) for the heat fluxes have the same shape as the fluxes themselves. The peak values of the axial coefficient are between -0.35 and -0.40 and are greater than for the radial coefficient ($+0.25 - +0.30$). Even when account has been taken of the error in the measurement, the maximum correlation coefficient is smaller than for the shear stress ($|R_{uv}| < 0.6$). Our values are similar to those of Tanaka & Yanagi (1983) in a bunsen-type premixed flame and are comparable with the results of Driscoll, Schefer & Dibble (1982) obtained in a non-premixed flame.

4. Discussion

Gradients of mean pressure in premixed flames can affect both the transport of the mean momentum of the reactants differently from that of the products, and the transport of turbulence energy and heat flux. The purpose of this discussion is to assess the importance of these effects relative to the other transport mechanisms and to examine the implications for calculation schemes.

4.1. *Mean momentum of reactants and products*

The terms in the transport of axial and radial momentum have been calculated from the results and are shown in figure 9(*a*, *b*) (normalized by $\rho_0 U_0^2$) for $x/D = 0.50$, 1.00 and 1.25 (note that the scales for the terms in the conservation equation of the radial momentum are half of those for the axial momentum). These stations correspond, approximately, to the maximum width of the recirculation bubble, a location part-way between this zone and the rear stagnation point and to the rear stagnation point itself. The mean pressure gradients have been found by addition and are dominated by the small difference between two large terms, namely the convection terms and the diffusion term in the balance of radial momentum. As a consequence these gradients are likely to be overestimated because of the errors in evaluating the axial gradients of momentum, due to the relatively large axial spacing between the measurement stations†. The pressure gradients represent an important source and sink of axial and radial momentum which is expected because of the large streamline curvature. Qualitatively, the pressure field is similar to that expected in the equivalent isothermal flow, for example that of Carmody (1964), and comparison with a related confined flow can be established from the calculations of McGuirk, Taylor & Whitelaw (1982). The consequences of the mean pressure gradients on the conditioned velocity field are analysed in the following paragraphs.

For $r/D < 0.5$, figure 9(*a*) shows that $\partial \bar{P}/\partial x$ is positive and decelerates the axial velocity component of the burned gases relative to the reactants with maximum differences of the order of $0.27 U_0$. For $r/D > 0.5$, with this value decreasing with the downstream distance, the axial pressure gradient is of similar magnitude but favourable and burned gases have higher velocities than reactants. The existence of large regions of the flow over which there is an adverse axial mean pressure gradient distinguishes these results from those of Moss (1980), Shepherd & Moss (1981),

† The axial gradients at $x/D = 0.50$ were evaluated by central differencing of data at $x/D = 0.375$ and 0.625; at $x/D = 1.00$ from data at $x/D = 0.625$ and 1.250; and at $x/D = 1.25$ from data at $x/D = 1.00$ and 1.50.

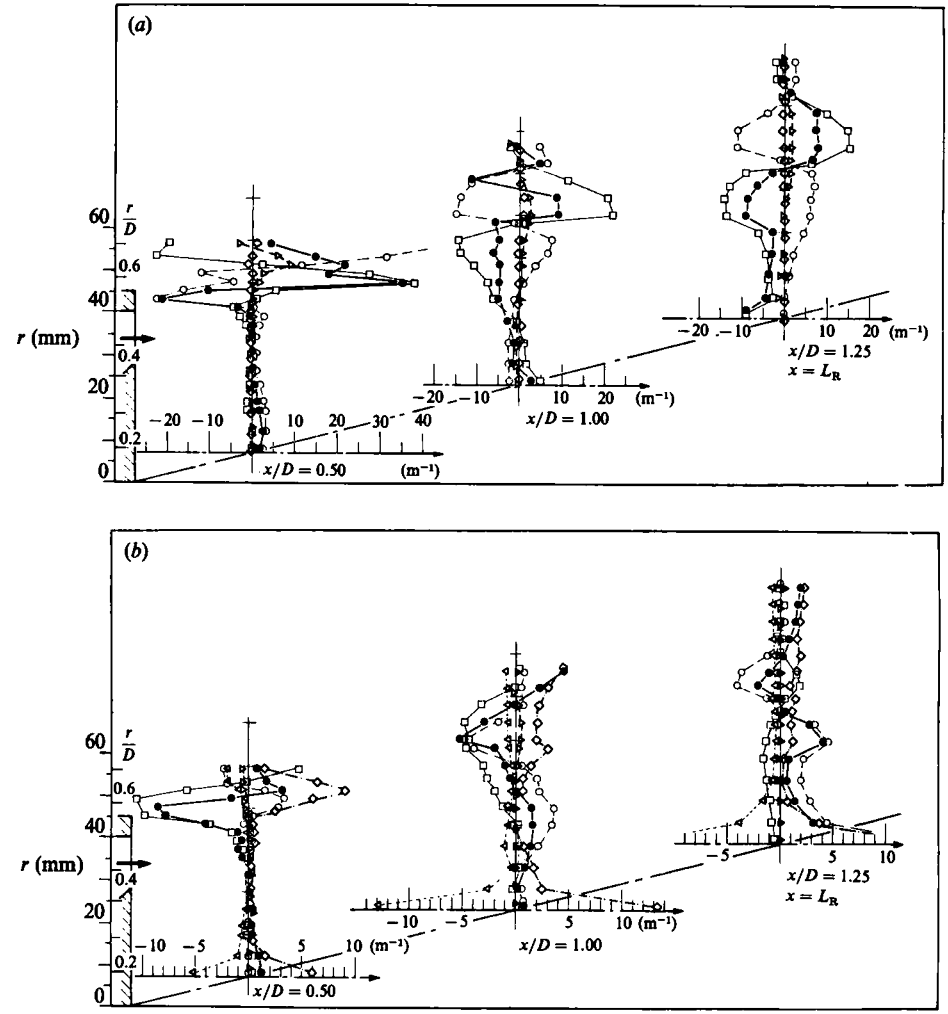

FIGURE 9. Radial profiles of the terms in the transport equations for mean momentum, normalized by $\rho_0 U_0^2$: all terms except the pressure gradient have been taken to the left-hand side of the equation.
(a) Axial momentum

—○— $\frac{\partial}{\partial x}\left(\bar{\rho}\tilde{U}^2\right)$; —□— $\frac{1}{r}\frac{\partial}{\partial r}\left(r\bar{\rho}\tilde{U}\tilde{V}\right)$; —◇— $\frac{\partial}{\partial x}\left(\bar{\rho}\widetilde{u''^2}\right)$; —▷— $\frac{1}{r}\frac{\partial}{\partial r}\left(r\bar{\rho}\widetilde{u''v''}\right)$;

—●— $-\frac{\partial\bar{P}}{\partial x}$ (By addition.)

(b) Radial momentum

—○— $\frac{1}{r}\frac{\partial}{\partial r}\left(r\bar{\rho}\tilde{V}^2\right)$; —□— $\frac{\partial}{\partial x}\left(\bar{\rho}\tilde{U}\tilde{V}\right)$; —◇— $\frac{1}{r}\frac{\partial}{\partial r}\left(r\bar{\rho}\widetilde{v''^2}\right)$; —▷— $\frac{\partial}{\partial x}\left(\bar{\rho}\widetilde{u''v''}\right)$;

—◁— $-\frac{1}{r}\bar{\rho}\widetilde{w''^2}$; —●— $-\frac{\partial\bar{P}}{\partial r}$ (By addition.)

Shepherd *et al.* (1982), Cheng & Ng (1983) and Cheng *et al.* (1984). In these references, the 'self-induced' pressure gradient accelerates the products across the flame front and fulfils the intuitive expectation that products have a higher velocity than reactants. Masuya & Libby (1981) have shown analytically that gradients of Reynolds shear stress can also differentially accelerate the dense reactants and light

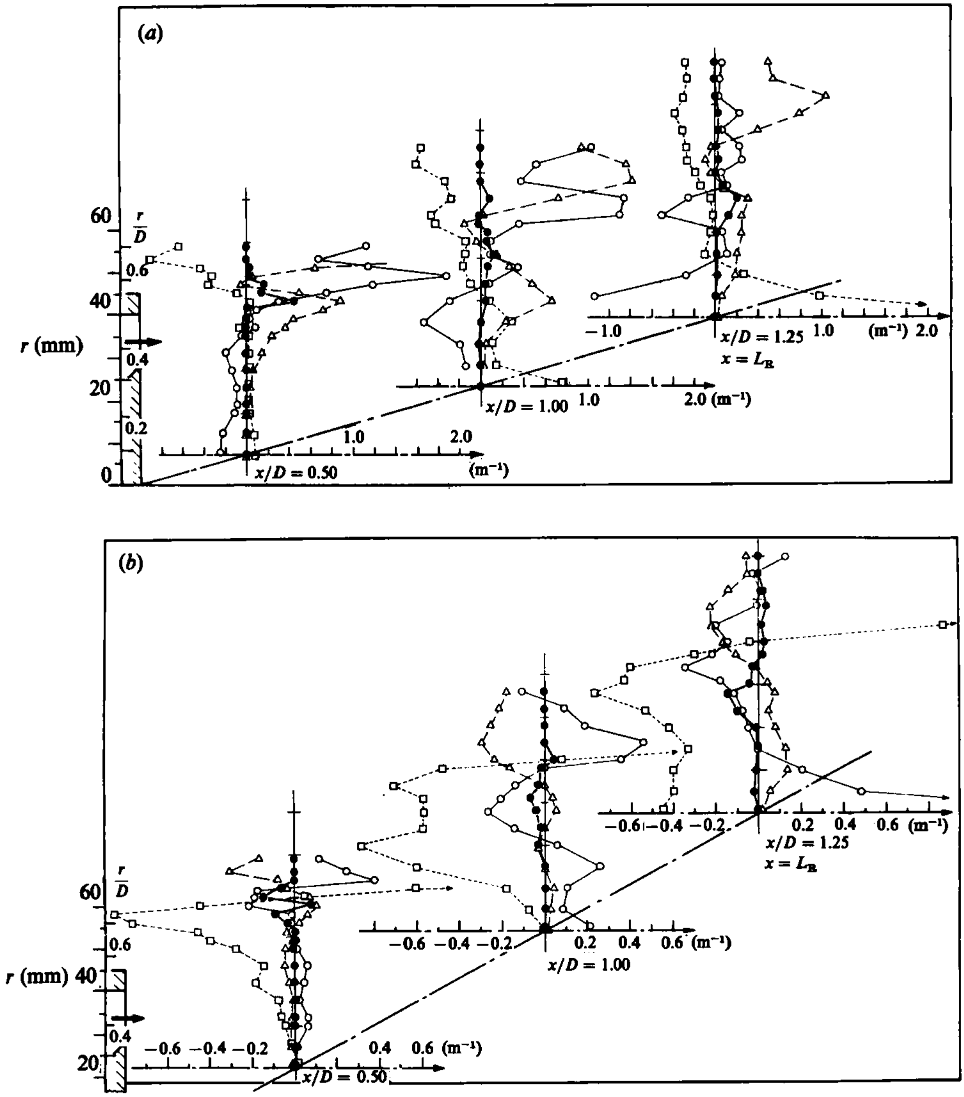

FIGURE 10. Radial profiles of the convection (left-hand side of equality sign) and production (right-hand side of equality sign) terms in the conservation equation for Reynolds stresses, normalized by $\rho_0 U_0^3$.

(*a*) Turbulent kinetic energy

Convection:

$$—\bigcirc— \frac{\partial}{\partial x}\left(\bar{\rho}\tilde{U}k\right)+\frac{1}{r}\frac{\partial}{\partial r}\left(r\bar{\rho}\tilde{V}k\right)$$

Production:

$$—\triangle— -\bar{\rho}\widetilde{u''v''}\left(\frac{\partial \tilde{U}}{\partial r}+\frac{\partial \tilde{V}}{\partial x}\right);\ —\square— -\bar{\rho}\widetilde{u''^2}\frac{\partial \tilde{U}}{\partial x}-\bar{\rho}\widetilde{v''^2}\frac{\partial \tilde{V}}{\partial r}-\frac{\tilde{V}}{r}\widetilde{w''^2};\ —\bullet— -\overline{u''}\frac{\partial \bar{P}}{\partial x}-\overline{v''}\frac{\partial \bar{P}}{\partial r}.$$

(*b*) Reynolds shear stress

Convection:

$$—\bigcirc— \frac{\partial}{\partial x}\left(\bar{\rho}\tilde{U}\widetilde{u''v''}\right)+\frac{1}{r}\frac{\partial}{\partial r}\left(r\bar{\rho}\tilde{V}\widetilde{u''v''}\right)$$

Production:

$$—\triangle— -\bar{\rho}\widetilde{u''v''}\left(\frac{\partial \tilde{U}}{\partial x}+\frac{\partial \tilde{V}}{\partial r}\right);\ —\square— -\bar{\rho}\widetilde{u''^2}\frac{\partial \tilde{V}}{\partial x}-\bar{\rho}\widetilde{v''^2}\frac{\partial \tilde{U}}{\partial r};\ —\bullet— -\overline{u''}\frac{\partial \bar{P}}{\partial r}-\overline{v''}\frac{\partial \bar{P}}{\partial x}.$$

products but here the gradients of shear stress are of secondary importance compared to the axial mean pressure gradient. The flux of radial momentum is influenced by both the radial gradients of mean pressure and $\widetilde{v''^2}$ and it is thus difficult to analyse the observation that the reactants have consistently smaller (larger negative) velocities than the products. The calculated radial pressure gradient is, as expected, favourable near the centreline and adverse near the shear layer surrounding the separation streamline. Also, the increased contribution of turbulent diffusion to the flux of radial momentum, compared with that for the axial momentum, agrees qualitatively with the isothermal measurements of MacLennan & Vincent (1982).

4.2. *Reynolds stresses*

The mean pressure gradient also appears in the transport equations for turbulent kinetic energy and for Reynolds shear stress and can act as either a source or a sink, as discussed by Bray *et al.* (1981) for premixed flames and Stårner & Bilger (1980) for non-premixed flames. The convection and production terms, normalized by $\rho_0\, U_0^3$, are shown in figure 10(*a*, *b*) with convection plotted so that a negative value represents a gain of turbulent kinetic energy. The value of $\overline{u_i''}$, the *time*-average of the density-weighted velocity fluctuation, is required in the evaluation of the source term that involves the gradient of mean pressure, i.e. $\overline{u_i''}\,\partial \bar{P}/\partial x_i$. This average was found from the exact equation (e.g. Bray *et al.* 1985)

$$\overline{u_i''} = \widetilde{u_i'' c''}\,\frac{\tau_{\mathrm{H}}}{1+\tilde{C}\tau_{\mathrm{H}}},$$

where $\tilde{C}$ and $\widetilde{u_i'' c''}$ are the measured density-weighted progress variable and the heat flux, respectively. The reader should bear in mind that the estimates of the terms in this figure, as well as in figures 9 and 11, are inevitably approximate because of the error in evaluating the spatial gradients. The values are sufficiently accurate, however, for the purpose of establishing the relative importance of the separate terms in the conservation equations.

Within the recirculation zone convection is the largest term, as in the reverse-flow zones of Chandrsuda & Bradshaw (1981) and Taylor & Whitelaw (1984). In the region of the separation streamline, upstream of stagnation (i.e. $x/D = 0.50$ and 1.00) the distribution of the various terms resembles that of the mixing layer of Wood & Bradshaw (1982), and upstream of the reattachment zone in the backstep flows of Chandrsuda & Bradshaw (1981) and Pronchick & Kline (1983): convection is small, production of turbulent energy is by shear stress, and turbulent diffusion and dissipation, although not plotted, are likely to be important and represent a loss. In common with the confined isothermal flow of Taylor & Whitelaw (1984), turbulence production is large in the vicinity of the free stagnation point, is comparable with the largest rate of production by shear stress at the same axial station but is through the interaction of normal stresses with normal strain. In the free-stream region, and in the plane of the stagnation zone (i.e. $0.15 < r/D < 0.40$), the present distribution resembles that of a turbulent jet (e.g. Tennekes & Lumley 1972) while the energy budget for the confined flow is similar to that of a turbulent wake because of the comparatively small value of the ratio $(\partial \tilde{U}/\partial x)/(\partial \tilde{U}/\partial r)$. In the core of the annular jet (i.e. $0.40 < r/D < 0.56$), turbulence production by normal and shear stresses is negative and convection is the largest term and represents a loss. Again, turbulent diffusion and dissipation are expected to balance these terms.

Turbulent production by $\overline{u_i''}\,\partial \bar{P}/\partial x_i$, although up to 50 % of the local production by shear stress around the reaction zone at $x/D = 0.50$, is a *minor* contribution throughout the flow. This is not surprising given the highly strained flow in the regions around the recirculation zone and is a further difference between this flow and the others mentioned in the previous sub-heading since the latter are only weakly strained.

The terms in the transport of shear stress, figure 10(*b*), show that production by $\overline{u_j''}\,\partial\bar{P}/\partial x_i$ is again the least important of the three source terms which are dominated over the whole length of the measurements by the interaction of normal stress with shear strain, i.e. $\widetilde{v''^2}\,\partial\tilde{U}/\partial r$, as in the isothermal flows cited above. Around the core of the annular jet, where $\widetilde{u''v''} \approx 0$, this term reverses from positive (in the outer flame zones) to negative (in the inner flame zones). By analogy with the isothermal flows, it is likely to be balanced by the pressure–strain redistribution terms.

4.3. *Turbulent heat flux*

The previous section (see also figure 2*b*) has shown that the turbulent-heat-flux vectors are predominantly directed along the isotherms rather than normal to these as would be expected from gradient-transport models of the kind used in non-reacting flows. Provided that chemical reaction occurs in 'thin flames' then the turbulent heat flux can be represented as

$$\widetilde{u_i''c''} = \tilde{C}(1-\tilde{C})\,(\bar{U}_{i\mathrm{P}} - \bar{U}_{i\mathrm{R}}). \tag{5}$$

To avoid confusion we note that, by analogy to (1) above, 'intermittency' is the only contributor to the turbulent heat flux and is therefore important: this statement should be contrasted to that for the unconditioned Reynolds stress.

As discussed in the introduction to §3, the above formula is an approximation, because of the finite thickness of the reaction zone, which is nevertheless useful in this discussion. The sign, and to a lesser extent the magnitude, of the heat flux is given by the difference in the product and reactant mean velocities. Based on the preceding discussion of the axial and radial velocities, the reasons for the large non-gradient heat flux in the axial direction $\widetilde{u''c''}$, and the much smaller gradient transport in the radial direction $\widetilde{v''c''}$, can be explained. The direction of the axial flux is towards the baffle for $r/D < 0.5$ because there $\bar{U}_{\mathrm{R}} > \bar{U}_{\mathrm{P}}$ for reasons stated above. For $r/D > 0.5$ (and for $x/D > 1.25$) the direction changes because there $\bar{U}_{\mathrm{R}} < \bar{U}_{\mathrm{P}}$, but the magnitude of the axial component is larger than that in the radial direction in both the zones because $|\bar{U}_{\mathrm{P}} - \bar{U}_{\mathrm{R}}| > |\bar{V}_{\mathrm{P}} - \bar{V}_{\mathrm{R}}|$. The radial flux is in the gradient sense only by virtue of the fact that $\bar{V}_{\mathrm{P}} > \bar{V}_{\mathrm{R}}$ everywhere. There does not appear to be any fundamental aerodynamic restriction that prevents $\bar{V}_{\mathrm{R}}$ becoming larger than $\bar{V}_{\mathrm{P}}$ except that, in that case, $\widetilde{v''c''}$ would represent counter-gradient heat transfer into the recirculation zone and it is not clear how a stable flame could exist. The conditions under which $\bar{V}_{\mathrm{R}}$ would become larger than $\bar{V}_{\mathrm{P}}$ are, presumably, values of equivalence ratio near unity when the density difference between products and reactants is largest and which therefore allows the maximum preferential acceleration between the two states.

Figure 11(*a*, *b*) shows the convection and production terms, normalized by $\rho_0 U_0^2$, and that production (both positive and negative) due to the pressure-gradient terms $-\overline{c''}\,\partial\bar{P}/\partial x_i$ is large over most of the flow. As for the value of $\overline{u_i''}$, the time-average of $\overline{c''}$ was found from the exact thermochemical relation (e.g. Bray *et al.* 1985)

$$\overline{c''} = \widetilde{c''^2}\,\frac{\tau_{\mathrm{H}}}{1+\tilde{C}\tau_{\mathrm{H}}},$$

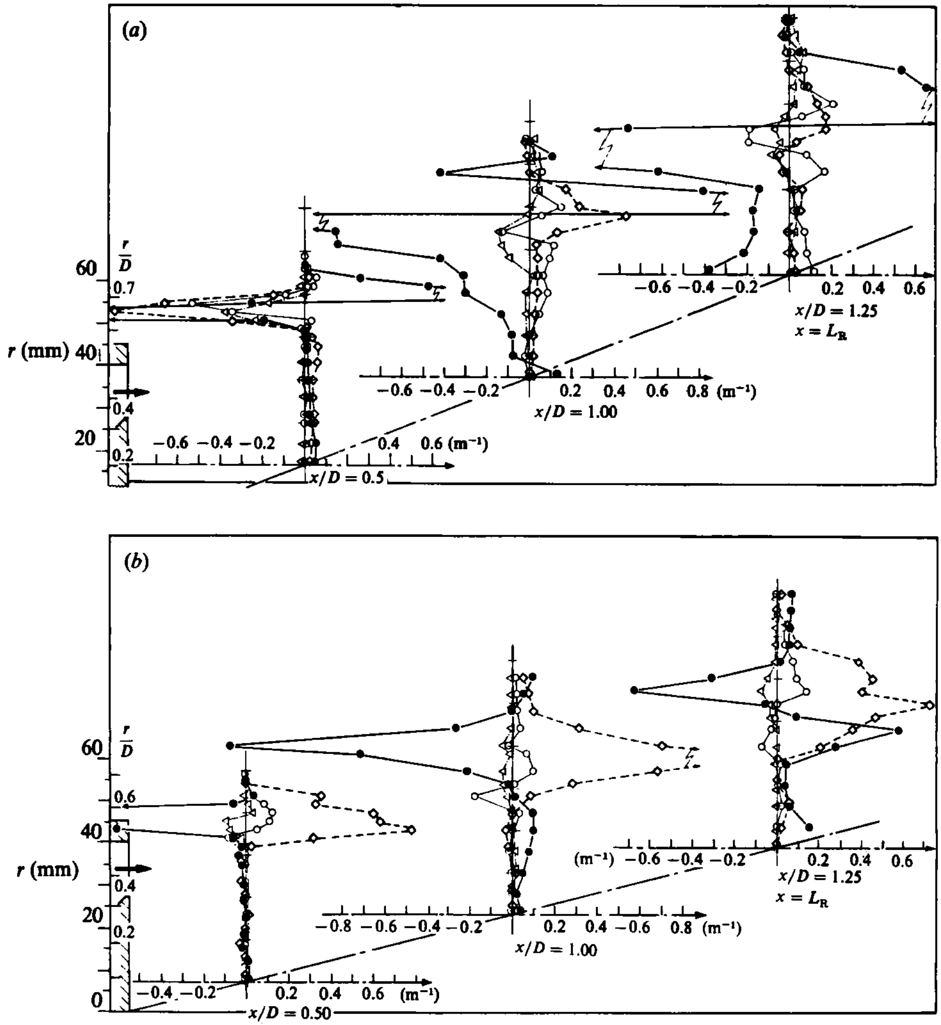

FIGURE 11. Radial profiles of the convection (left-hand side of equality sign) and production (right-hand side of equality sign) terms in the conservation equations for turbulence heat transfer rate, normalized by $\rho_0 U_0^3$.

(*a*) Axial heat flux

Convection:

$$—\bigcirc— \frac{\partial}{\partial x}\left(\bar{\rho}\tilde{U}\widetilde{u''c''}\right)+\frac{1}{r}\frac{\partial}{\partial r}\left(r\bar{\rho}\tilde{V}\widetilde{u''c''}\right)$$

Production:

$$—\triangleleft— -\bar{\rho}\widetilde{u''c''}\frac{\partial\tilde{U}}{\partial x}-\bar{\rho}\widetilde{v''c''}\frac{\partial\tilde{U}}{\partial r};\; —\diamond— -\bar{\rho}\widetilde{u''^2}\frac{\partial\tilde{C}}{\partial x}-\bar{\rho}\widetilde{u''v''}\frac{\partial\tilde{C}}{\partial r};\; —\bullet— -\overline{c''}\frac{\partial\bar{P}}{\partial x}.$$

(*b*) Radial heat flux

Convection:

$$—\bigcirc— \frac{\partial}{\partial x}\left(\bar{\rho}\tilde{U}\widetilde{v''c''}\right)+\frac{1}{r}\left(\frac{\partial}{\partial r}r\bar{\rho}\tilde{V}\widetilde{v''c''}\right)$$

Production:

$$—\triangleleft— -\bar{\rho}\widetilde{u''c''}\frac{\partial\tilde{V}}{\partial x}-\bar{\rho}\widetilde{v''c''}\frac{\partial\tilde{V}}{\partial r};\; —\diamond— -\bar{\rho}\widetilde{v''^2}\frac{\partial\tilde{C}}{\partial r}-\bar{\rho}\widetilde{u''v''}\frac{\partial\tilde{C}}{\partial x};\; —\bullet— -\overline{c''}\frac{\partial\bar{P}}{\partial r}.$$

where $\tilde{C}$ and $\widetilde{c''^2}$ were measured. In the transport equation for axial flux the term is dominant and must be balanced mainly by turbulent diffusion. For the transport of radial flux this term is similar in magnitude to production through the interaction of Reynolds stress with the spatial gradient of the mean value of the reaction progress variable (i.e. mainly $-\widetilde{v''^2}\,\partial\tilde{C}/\partial r$), but is generally of the opposite sign. The sign of $\widetilde{v''c''}$ is thus a balance between two large, but competing, source terms.

Finally, we briefly consider the implications of our results for the calculation of premixed flames using turbulence models. The most recent work in this field is that of Bray *et al.* (1985) who propose the solution of fifteen equations (for the dependent variables, P, U_i, C, $\widetilde{u_i''u_j''}$, $\widetilde{u_i''c''}$ and $\tilde{\epsilon}$, the mass-averaged rate of dissipation of turbulent kinetic energy). One motivation for developing a model at the level of transport equations for the Reynolds stresses and turbulent heat fluxes, rather than at the level of a turbulent-viscosity closure, is to avoid as far as possible the use of gradient hypotheses and to represent directly those processes arising from variable density. Our experimental evidence supports the case for calculating the heat fluxes from the transport equations, because the source terms involving the mean pressure gradient are either large or dominant. It is reasonable to expect that the representation of the fluxes by mean gradient transport of the type developed for isothermal flows – for which the conservation equations for second-moment quantities have no source terms involving the mean pressure gradient – will be unsuccessful. It is more questionable whether the presence of the 'unusual' source term ($\overline{u_i''}\,\partial\bar{P}/\partial x_i$), alone, is sufficient cause for progressing to the solution of the transport equations, because the direct contribution to the budget is smaller than the source terms due to the interaction of Reynolds stress with the rate of strain. Also, at least in non-reactive flow, recent calculations with Reynolds-stress models have not provided significantly better representations of the velocity field in the lee of a bluff body (e.g. McGuirk, Papadimitriou & Taylor 1985) than a two-equation turbulence model. It is likely, however, that this level of complexity for the Reynolds stress will be needed if the heat-flux terms are to be obtained from a second-moment closure.

5. Conclusions

Velocity and temperature measurements have provided information about the turbulence characteristics of highly strained disk-stabilized premixed flames in an unconfined arrangement. The flames are non-planar and oblique to the oncoming reactants and their temperature distributions, although affected by intermediate burning states, reveal predominantly biomodal characteristics. The following is a summary of the more important findings and conclusions of this work.

(i) (*a*) The interaction between gradients of mean pressure and the large density fluctuations that occur in the flame represents the largest source terms in the transport equations for the turbulent heat fluxes but is less important in the conservation of the Reynolds stresses and turbulent kinetic energy.

(i) (*b*) The turbulent heat flux is, as expected, large in the shear layer where the temperature fluctuations are large. The direction of the flux is not, however, aligned with the direction of the gradient of the mean temperature. The axial component is dominated by the source term $\overline{c''}\,\partial\bar{P}/\partial x$, which is presumably balanced by turbulent diffusion. The magnitude of the radial component, which is ultimately responsible for assuring the stabilization of the flame, is determined by the competing effects of the source terms $\overline{c''}\,\partial\bar{P}/\partial r$ and $\widetilde{v''^2}\,\partial\tilde{C}/\partial r$.

(ii) The velocity characteristics may be associated with the concept of thin-flame turbulent burning, since the moments of velocity are made up principally of the separate contributions from the reactants and products. The existence of heat transfer in the flame thus depends on the difference between the mean velocities of the reactant and product gases.

(ii) (*a*) In the shear layer, for $r/D < 0.50$, the mean axial velocity of the reactants is larger than that of the products by up to $0.27 U_0$. This is due to the local preferential deceleration of low-density hot products relative to high-density cold reactants by the adverse, axial mean pressure gradient.

(ii) (*b*) In the outer flame zones, for $r/D > 0.5$, the axial pressure gradient is favourable and accelerates the burned gases relative to the reactants with maximum differences of the order of $0.05 U_0$.

(ii) (*c*) Over the whole area of the measurements, the hot products are deflected outwards (by up to 5°) relative to the reactants but it is not possible to relate this observation with the sign of the radial pressure gradient, in contrast to (ii) (*a*) above for the axial component of velocity.

(ii) (*d*) The conditioned Reynolds stresses within reactants and products are the main contribution to the respective unconditioned stresses and reveal characteristics different from those reported in the literature. The magnitude of normal and shear stresses of the products are higher than those of the reactants except for a small area around the core of the annular jet where turbulence is removed, rather than produced, by shear stress.

(iii) The velocity characteristics of the combusting flow are qualitatively similar to those of the equivalent isothermal flow. Combustion has, however, increased the recirculation length by 67 %, the maximum reverse velocity by 18 % and the maximum value of the turbulent kinetic energy by 32 %: it has decreased the recirculating mass flow rate by 51 %.

The anisotropy of Reynolds stress around the reverse-flow boundary is particularly high and the maximum turbulent kinetic energy lies near the rear stagnation point owing to comparatively high radial intensities. Inspection of the terms in the conservation equation of turbulent kinetic energy confirms that this behaviour is associated with the interaction between normal stress and normal strain. The locations of zero shear stress do not coincide with those of zero mean velocity gradient, with increased differences in the combusting flow.

The results also indicate that turbulent diffusion and dissipation are likely to be important in the balance of turbulent kinetic energy, particularly near stagnation and around the core of the annular jet.

(iv) The evidence suggests that the calculation of $\widetilde{u_i'' c''}$ in this type of turbulent premixed flame must be found from a modelled transport equation rather than from a turbulent-viscosity hypothesis.

We would like to record our thanks to Professor P. A. Libby and Dr W. P. Jones for many useful discussions and to Mr J. R. Laker for his invaluable technical assistance. We acknowledge the financial support provided by the Science and Engineering Research Council and the Ministry of Defence of the United Kingdom. A. M. K. P. T. is supported by the award of a Royal Society 1983 University Research Fellowship.

REFERENCES

ABRAHAM, J., WILLIAMS, F. A. & BRACCO, F. V. 1985 A discussion of turbulent flame structure in premixed charges. *SAE, p-156: Intl Cong. and Exp. on Engine combustion analysis – new approaches, Detroit, Michigan, Feb./March, 1985*, pp. 27–42.

BILL, R. G., NAMER, I., TALBOT, L. CHENG, R. K. & ROBBEN, F. 1982 Density fluctuations of flames in grid-induced turbulence. *Combust. Flame* **44**, 277–285.

BALLANTYNE, A., BOON, D. J. & MOSS, J. B. 1976 Measurements of fluctuating temperature on open diffusion flames employing fine wire thermocouples. *Mem.* 76/3. Department of Aeronautics and Astronautics, University of Southampton.

BRADBURY, L. J. S. 1976 Measurements with a pulsed-wire and a hot-wire anemometer in the highly turbulent wake of a normal flat plate. *J. Fluid Mech.* **77**, 473–497.

BRADLEY, D. & MATTHEWS, K. I. 1968 Measurements of high gas temperature with fine wire thermocouple. *J. Mech. Engng Sci.* **10**, 299–305.

BRADSHAW, P., FERRISS, D. H. & ATWELL, N. P. 1967 Calculation of boundary layer development using the turbulent energy equation. *J. Fluid Mech.* **28**, 593–616.

BRADSHAW, P. & WONG, F. Y. F. 1972 The reattachment and relaxation of a turbulent shear layer. *J. Fluid Mech.* **52**, 113–135.

BRAY, K. N. C. 1980 Turbulent flows with premixed reactants. In *Turbulent Reacting Flows* (ed. P. A. Libby & F. A. Williams), pp. 115–183. Springer.

BRAY, K. N. C., LIBBY, P. A., MASUYA, G. & MOSS, J. B. 1981 Turbulence production in premixed turbulent flames. *Combust. Sci. Tech.* **25**, 127–140.

BRAY, K. N. C., LIBBY, P. A. & MOSS, J. B. 1985 Unified modelling approach for premixed turbulent combustion – Part I: General formulation. *Combust. Flame* **61**, 87–102.

CARMODY, T. 1964 Establishment of the wake behind a disc. *Trans. ASME* D: *J. Basic Engng* **86**, 869–882.

CASTRO, I. P. 1985 Time-domain measurements in separated flows. *J. Fluid Mech.* **150**, 183–201.

CASTRO, I. P. & BRADSHAW, P. 1976 The turbulence structure of a highly curved mixing layer. *J. Fluid Mech.* **73**, 265–304.

CHANDRSUDA, C. & BRADSHAW, P. 1981 Turbulence structure of a reattaching mixing layer. *J. Fluid Mech.* **110**, 171–194.

CHENG, R. K. 1984 Conditional sampling of turbulence intensities and Reynolds stresses in a premixed turbulent flame. *Combust. Sci. Tech.* **41**, 109–142.

CHENG, R. K. & NG, T. T. 1983 Velocity statistics in premixed turbulent flames. *Combust. Flame* **52**, 185–202.

CHENG, R. K., TALBOT, L. & ROBBEN, F. 1984 Conditional velocity statistics in premixed CH_4–air, C_2H_4–air turbulent flames. *The 20th Symp. (Intl) on Combustion*, pp. 453–463. The Combustion Institute, Pittsburgh, PA 15213.

CHEVRAY, R. & TUTU, N. K. 1978 Intermittency and preferential transport of heat in a round jet. *J. Fluid Mech.* **88**, 133–160.

CLARE, H., DURÃO, D. F. G., MELLING, A. & WHITELAW, J. H. 1976 Investigation of a V-gutter stabilised flame by laser anemometry and schlieren photography. *AGARD-CP*-19, Paper No. 26.

COLLIS, D. C. & WILLIAMS, M. J. 1959 Two dimensional convection from heated wires at low Reynolds number. *J. Fluid Mech.* **6**, 357–384.

DAKOS, T., VERRIOPOULOS, C. A. & GIBSON, M. M. 1984 Turbulent flow with heat transfer in plane and curved wall jets. *J. Fluid Mech.* **145**, 339–360.

DRISCOLL, J. F., SCHEFER, R. W. & DIBBLE, R. W. 1982 Mass fluxes $\overline{\rho''u''}$ and $\overline{\rho v''}$ measured in a turbulent nonpremixed flame. *19th Symp. (Intl) on Combustion*, pp. 477–485. The Combustion Institute, Pittsburgh, PA 15213.

DRIVER, D. M. & SEEGMILLER, H. L. 1982 Features of a reattaching turbulent shear layer subject to an adverse pressure gradient. *AIAA J.* **23**, 163–171.

DURÃO, D. F. G., DURST, F. & FIRMINO, F. J. C. 1984 Velocity characteristics of the flow around cones. *2nd Intl Symp. on Applications of Laser Anemometry to Fluid Mechanics, Lisbon, July 1984*, paper 15.2.

Durão, D. F. G. & Whitelaw, J. H. 1978 Velocity characteristics of the flow in the near wake of a disk. *J. Fluid Mech.* **85**, 369–385.

Durst, F. & Kleine, R. 1973 Geschwindigskeitsmessungen in Turbulenten Vormischflammen mitels Laserstrahl-anemometer. *Gas Waerme International* **22**, 484–492.

Etheridge, D. W. & Kemp, P. H. 1978 Measurements of turbulent flow downstream of a rearward-facing step. *J. Fluid Mech.* **86**, 545–566.

Fujii, S. & Eguchi, K. 1981 A comparison of cold and reacting flows around a bluff-body flame stabilizer. *AIAA J.* **19**, 1438–1442.

Fujii, S., Gomi, M. & Eguchi, K. 1978 Cold flow tests of a bluff body flame stabilizer. *Trans. ASME* I: *J. Fluids Engng* **100**, 232–332.

Gibson, M. M. & Verriopoulos, C. 1984 Turbulent boundary layer on a mildly curved convex surface. Part 2: Temperature field measurements. *Exp. Fluids* **2**, 73–80.

Glass, M. & Bilger, R. W. 1978 The turbulent jet diffusion flame in a co-flowing stream – some velocity measurements. *Combust. Sci. Tech.* **18**, 165–177.

Harsha, P. T. & Lee, S. C. 1970 Correlation between turbulent shear stress and turbulent kinetic energy. *AIAA J.* **8**, 1508–1510.

Heitor, M. V. 1985 Experiments in turbulent reacting flows. PhD thesis, University of London.

Heitor, M. V., Taylor, A. M. K. P. & Whitelaw, J. H. 1984 Influence of confinement on combustion instabilities of premixed flames stabilised on axisymmetric baffles. *Combust. Flame* **57**, 109–121.

Heitor, M. V., Taylor, A. M. K. P. & Whitelaw, J. H. 1985 Simultaneous velocity and temperature measurements in a premixed flame. *Exp. Fluids*, **3**, 323–339. Also, *Proc. ASME 105th Ann. Winter Meeting, New Orleans, 9–13 Dec. 1984.*

Johnson, B. V. & Bennett, J. C. 1983 Mass and momentum turbulent transport experiments with confined co-axial jets. *Proc. 4th Symp. on Turbulent Shear Flows*, pp. 18.4–18.19. Karlsruhe 1983. Springer.

Kim, J., Kline, S. J. & Johnston, J. P. 1978 Investigation of a reattaching turbulent shear layer: flow over a backward-facing step. *Trans. ASME* I: *J. Fluids Engng* **102**, 302–308.

Libby, P. A. 1985 Theory of normal premixed turbulent flames revisited. *Prog. Energy Combust. Sci.* **11**, 83–96.

MacLennan, A. S. M. & Vincent, J. H. 1982 Transport in the near aerodynamic wakes of flat plates. *J. Fluid Mech.* **120**, 185–197.

McGuirk, J. J., Papadimitriou, C. & Taylor, A. M. K. P. 1985 Reynolds stress model calculations of two-dimensional plane and axisymmetric recirculating flows. *5th Symp. on Turbulent Shear flows, Cornell, 1985.*

McGuirk, J. J., Taylor, A. M. K. P. & Whitelaw, J. H. 1982 An assessment of numerical diffusion in upwind difference calculations of turbulent recirculating flows. In *Turbulent Shear Flows*, vol. 3 (ed. L. J. S. Bradbury, F. Durst, B. E. Launder, F. W. Schmidt & J. H. Whitelaw), pp. 206–224, Springer.

McLaughlin, D. K. & Tiederman, W. G. 1973 Biasing correction for individual realisation of laser anemometer measurements in turbulent flows. *Phys. Fluids* **16**, 2082–2088.

Masuya, G. & Libby, P. A. 1981 Non-gradient theory for oblique turbulent flames with premixed reactants. *AIAA J.* **19**, 1590–1599.

Moffat, R. J. 1958 Designing thermocouples for response rate. *Trans. ASME* **80**, 257–262.

Moss, J. B. 1980 Simultaneous measurements of concentration and velocity in an open turbulent flame. *Combust. Sci. Tech.* **22**, 119–129.

Pronchick, S. W. & Kline, S. J. 1983 An experimental investigation of the structure of a turbulent reattaching flow behind a backward-facing step. *Rep.* MD-42, Thermoscience Division, Dept. Mech. Engng, Stanford University, Stanford, California.

Ribeiro, M. M. & Whitelaw, J. H. 1980*a* The structure of turbulent jets. *Proc. R. Soc. Lond.* A **370**, 281–301.

Ribeiro, M. M. & Whitelaw, J. H. 1980*b* Coaxial jets with and without swirl. *J. Fluid Mech.* **96**, 769–775.

Shepherd, I. G. & Moss, J. B. 1981 Measurements of conditioned velocities in a turbulent premixed flame. *AIAA J.* **20**, 566–569.

SHEPHERD, I. G. & MOSS, J. B. 1983 Characteristic scales for density fluctuations in a turbulent premixed flame. *Combust. Sci. Tech.* **33**, 231–243.

SHEPHERD, I. G., MOSS, J. B. & BRAY, K. N. C. 1982 Turbulent transport in a confined premixed flame. *19th Symp. (Intl) on Combustion*, pp. 423–431. The Combustion Institute, Pittsburgh, PA 15213.

STÅRNER, S. H. 1983 Joint measurements of radial velocity and scalars in turbulent diffusion flame. *Combust. Sci. Tech.* **30**, 145–169.

STÅRNER, S. H. & BILGER, R. W. 1980 LDA measurements in a turbulent diffusion flame with axial pressure gradient. *Combust. Sci. Tech.* **21**, 259–276.

STÅRNER, S. H. & BILGER, R. W. 1981 Measurement of scalar-velocity correlations in a turbulent diffusion flame. In *Proc. 18th Symp. (Intl) on Combustion*, pp. 921–930. The Combustion Institute, Pittsburgh, PA 15213.

TANAKA, H. & YANAGI, T. 1983 Cross-correlation of velocity and temperature in a premixed turbulent flame. *Combust. Flame* **51**, 183–191.

TAYLOR, A. M. K. P. & WHITELAW, J. H. 1980 Velocity and temperature measurements in a premixed flame within an axisymmetric combustor. *AGARD-CP*-281, Paper No. 14.

TAYLOR, A. M. K. P. & WHITELAW, J. H. 1984 Velocity characteristics in the turbulent near wake flows of confined axisymmetric bluff bodies. *J. Fluid Mech.* **139**, 391–416.

TENNEKES, H. & LUMLEY, J.L. 1972 *A First Course in Turbulence.* The MIT Press.

TOWNSEND, A. A. 1976 *The Structure of Turbulent Shear Flow* (2nd edn). Cambridge University Press.

VINCKIER, J. & VAN TIGGELEN, A. 1968 Structure and burning velocity of turbulent premixed flames. *Combust. Flame* **12**, 561–568.

WESTENBERG, A. A., BERL, W. G. & RICE, J. G. 1955 Studies of flow and mixing in the recirculation zone of baffle-type flameholders. *Proc. Gas Dynamics on Aerothermochemistry, Northwestern Univ., August 1955*, pp. 211–219.

WILLIAMS, F. A. 1984 Some aspects of the interaction between turbulent flows and combustion processes. Eastern States Section, The Combustion Institute, Dec., 1984.

WINTERFELD, G. 1965 On processes of turbulent exchange behind flame holders. *10th Symp. (Intl) on Combustion*, pp. 1265–1275. The Combustion Institute, Pittsburgh, PA 15213.

WOOD, D. H. & BRADSHAW, P. 1982 A turbulent mixing layer constrained by a solid surface. Part 1. Measurements before reaching the surface. *J. Fluid Mech.* **122**, 57–89.

YANTA, W. J. & SMITH, R. A. 1978 Measurements of turbulence-transport properties with a laser-Doppler velocimeter. *AIAA paper no.* 73-169, presented at 11th Aerospace Science Meeting, Washington.

YOSHIDA, A. 1981 Experimental study of wrinkled laminar flame. *18th Symp. (Intl) on Combustion*, pp. 931–939. The Combustion Institute, Pittsburgh, PA 15213.